

Timing noise, glitches and the braking index of PSR B0540–69

G. Cusumano¹, E. Massaro^{2,3}, T. Mineo¹

¹ Istituto di Astrofisica Spaziale e Fisica Cosmica - Sezione di Palermo, CNR, Via Ugo La Malfa 153, I-90146, Palermo, Italy

² Dipartimento di Fisica, Università La Sapienza, Piazzale A. Moro 2, I-00185, Roma, Italy

³ Istituto di Astrofisica Spaziale e Fisica Cosmica - Sezione di Roma, CNR, Via del Fosso del Cavaliere, I-00100 Roma, Italy

Received.:; accepted:.

Abstract. We report a pulse-time history of PSR B0540–69 based on the analysis of an extended Data set including ASCA, BeppoSAX and RXTE observations spanning a time interval of about 8 years. This interval includes also the epoch of the glitch episode reported by Zhang et al. (2001). Our analysis shows the presence of a relevant timing noise and does not give a clear evidence of the glitch occurrence. We performed an accurate evaluation of the main timing parameters, ν , $\dot{\nu}$ and $\ddot{\nu}$ and derived a mean braking index of $n = 2.125 \pm 0.001$ quite different from the lower value found by Zhang et al. (2001), but in rather good agreement with other several values reported in the literature.

Key words. stars: neutron – pulsars: individual: PSR B0540–69 – X-rays: stars

1. Introduction

PSR B0540–69 was discovered in the soft X-rays by Seward et al. (1984) in a field of the Large Magellanic Cloud observed with the Einstein Observatory. Pulsations at optical frequencies were soon detected by Middleditch & Pennypacker (1985) with a mean pulsed magnitude of 22.5. In the radio band PSR B0540–69 is a quite faint source and pulsed signals were first observed only in 1989–90 (Manchester et al. 1993).

PSR B0540–69 is one of the youngest rotation powered pulsars. It has a period of about 50 ms and a large period derivative of $4.79 \times 10^{-13} \text{ s s}^{-1}$, comparable to that of the Crab pulsar, and a spin down age of about 1500 years. The pulse shape, at X and optical wavelengths, is broad and almost sinusoidal. Several estimates of the braking index n have been reported in the literature (see Boyd et al. 1995 for a compilation of older results) ranging from 2.01 ± 0.02 (Manchester & Peterson 1989; Nagase et al. 1990) to 2.74 ± 0.10 (Ögelman & Hasinger 1990). Deeter et al. (1998) analyzed an extended set of GINGA observations and found a braking index of 2.08 ± 0.02 . This result was substantially confirmed by Mineo et al. (1999), who combining a BeppoSAX frequency measurement with earlier ASCA results derived a value of 2.10 ± 0.1 . A recent analysis of all ASCA pointed observations gave a braking index of 2.10 (Hirayama et al. 2002). A glitch

in the timing history of PSR B0540–69, the only one reported up to now for this young Crab-like pulsar, has been recently pointed out by Zhang et al. (2001). These authors based their analysis on a collection of RXTE observations, spanning 1.2 years. The approximate epoch of the glitch, according to their estimates, occurred on MJD 51325 ± 45 and the change in frequency and its first derivative were $\Delta\nu/\nu = (1.90 \pm 0.04) \times 10^{-9}$ and $\Delta\dot{\nu}/\dot{\nu} = (8.5 \pm 0.07) \times 10^{-5}$, respectively. Zhang et al. (2001) measured also the braking index after the glitch which resulted equal to 1.81 ± 0.07 , significantly lower than the values reported from other analyses.

In this paper we present an exhaustive timing analysis of PSR B0540–69 performed on RXTE data set spanning about 5 years. In particular, we extend the set of RXTE observations used by Zhang et al. (2001), adding more observations for a total time interval of about 3 years before and 2 years after the epoch of the glitch episode claimed by these authors. Moreover, to further increase the time interval data set, public ASCA and BeppoSAX observations are also included in the analysis extending the length up to about 8 years.

2. Observation and Data Reduction

The RXTE observations considered in the present paper were performed between March 8, 1996 and March 14, 2001. We used only data obtained with the PCA (Jahoda et al. 1996) accumulated in “Good Xenon” telemetry

Send offprint requests to: G. Cusumano: giancarlo.cusumano@pa.iasf.cnr.it

mode, time-tagged with a $1\mu\text{s}$ accuracy with respect to the spacecraft clock, which is maintained to the UTC better than $100\ \mu\text{s}$. The pulsar position inside the instrument Field of View (FoV) is different in the various pointings and ranges between 0 and 25 arcminutes far from the centre. Following Zhang et al. (2001) we considered only events with pulse-height channels between 5 and 50, corresponding to the 2–18 keV energy interval. Furthermore, we verified that the selection of all PCA detector layers, instead of those from the top layer only, increased significantly the S/N ratio of the pulsation and adopted this choice for all the observations.

PSR B0540-69 was observed by ASCA (Tanaka et al. 1994) 14 times between 1993-06-13 and 1999-11-03. Only data from GIS (Ohashi et al. 1996, Makishima et al. 1996) were used in our analysis. The pulsar position inside the FoV ranges between 0 and 22 arcminutes off-axis. The Narrow Field Instruments (NFIs) onboard BeppoSAX (Boella et al. 1997a) observed PSR B0540-69 five times between 1996-10-26 and 2000-02-19. We considered only data from MECS (Boella et al. 1996) because they are in the same energy range used for the analysis of the other two satellites. The position of the source inside the instrument FoV lies between 0 and 17 arcminutes. Data from both imaging instruments (GIS and MECS) were extracted from regions centered at the source position and the shapes and sizes of these regions were optimized for each observation, depending upon the different off-axis locations, to achieve the highest S/N ratio. The log of all these observations is given in Table A1, available in electronic form at CDS (<http://cdsweb.u-strasbg.fr/>).

3. Timing analysis and pulse profile

3.1. Frequencies and derivatives evaluation

The UTC arrival times of all selected events were first converted to the Solar System Barycentre using the (J2000) pulsar position $\alpha = 5^{\text{h}}40^{\text{m}}10^{\text{s}}.95$ and $\delta = -69^{\circ}19'55''.1$ (Caraveo et al. 1992) and the JPL2000 ephemeris (DE200; Standish 1982). For each observation we searched the pulsed frequency ν using the folding technique in a range centered at the values computed by means of the pulsar ephemeris reported by Deeter et al. (1999). The central time of each observation was chosen as reference epoch and the corresponding frequency was estimated by fitting the χ^2 peak with a gaussian profile. Both these data are listed in Table A1 (columns 2 and 7, respectively). Frequency errors at $1\ \sigma$ level were computed with two different methods. The first evaluation was performed computing the frequency interval corresponding to a unit decrement with respect to the maximum in the χ^2 curve ($err = \nu(\chi_{max}^2) - \nu(\chi_{max}^2 - 1)$). In the second method we produced a template profile folding the longest RXTE observation (rows 33+34 in Table A1) with its best frequency (see Fig.1). The zero phase was taken at the centre of the peak. Then, we compared the folded profiles of other pointings with an accurate analytical model of

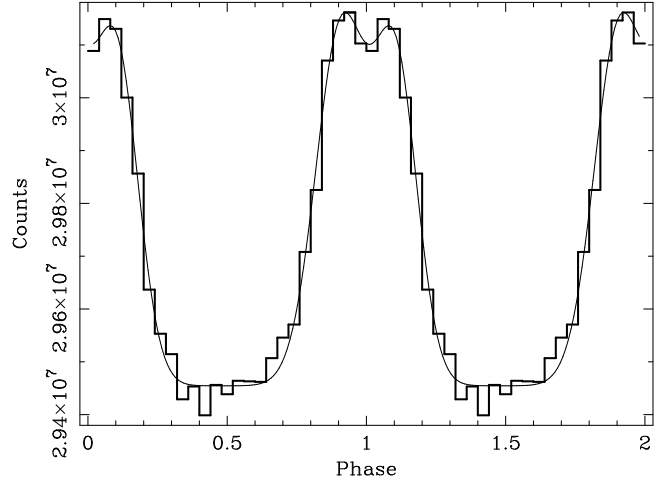


Fig. 1. The (2–18 keV) pulse profile of PSR B0540–69 in 25 phase bins. The analytical model used as template for the timing analysis is also shown.

the template changing the frequency within the searching range and computed the relative χ^2 values. For a correct comparison we subtracted the off-pulse levels and normalized the total pulsed counts. The frequency uncertainties were then set equal to the frequency interval corresponding to an increase of the χ^2 by a unit with respect to the minimum in the curve ($err = \nu(\chi_{min}^2 + 1) - \nu(\chi_{min}^2)$). No significant difference was found between the error estimates obtained with the two methods, we then considered as proper statistical uncertainties of the pulsar frequencies those computed with the first one (column 8). All errors, thereafter, refer to one standard deviation. The times of arrival (TOA), referred to the peak centre, were also determined for all RXTE observations by cross-correlating the folded profiles with the analytical model of the template. The resulting phase offset was added to the central time of the observation. Errors on TOAs were assumed equal to the statistical uncertainties of the peak centre derived from a best fit of the pulse profile. TOA and errors are reported in Table A1 (columns 5 and 6.)

A first estimate of the frequency derivatives was obtained by the best fit of the frequency history listed in Table A1 with the second-degree polynomial:

$$\nu(t) = \nu_0 + \dot{\nu}_0(t - t_0) + \frac{1}{2}\ddot{\nu}_0(t - t_0)^2. \quad (1)$$

This procedure was first applied separately to the two ASCA+BeppoSAX and RXTE frequency sets and the resulting parameters' values were found in a good agreement within their uncertainties. We then evaluated the ephemeris for the whole set of data (RXTE+ASCA+BeppoSAX); a summary of these results is given in Table 1. For easy comparison, the same reference epoch (t_0) was taken, in all the fittings, equal to MJD 50372.5481748585. Fig. 2 shows the residuals obtained fitting the entire frequency set with Eq.(1): the number of frequency values in excess of 2 standard de-

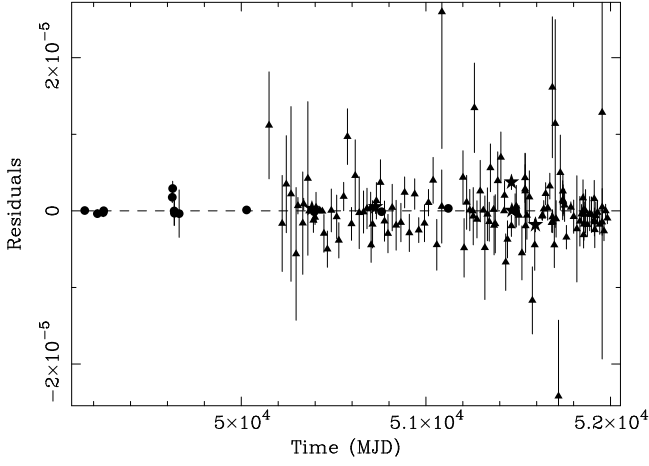


Fig. 2. Residuals of the best fit of the frequencies obtained by the folding technique with the polynomial formula of Eq.(1). Triangles represents RXTE data, circle ASCA data and stars BeppoSAX data.

viations is about 6% of the total, confirming the right evaluation of the frequency errors.

3.2. Pulse phase analysis

The precision of the timing parameters can be enhanced by maintaining a pulse coherence over the entire time interval covered by the observations. This analysis was performed only on the RXTE data. The BeppoSAX timing, in fact, does not maintain the indispensable accuracy to the UTC, fundamental to apply a coherent phase analysis. The ASCA observations are rather sparse and the systematics in the absolute time assignment (Hirayama et al. 1996) makes more complicated the proper phase recycle correction.

The arrival times of every event for RXTE observations were folded by using the values of ν_o , $\dot{\nu}_o$, $\ddot{\nu}_o$ reported in Table 1 (line 3). Phase shifts of the pulse profiles, expected because of the ephemeris accuracy, were computed for all observations by a cross-correlation with the analytical model of the template (Fig. 1). Phase errors were taken equal to the TOA uncertainties multiplied by the corresponding frequencies. Throughout this paper phases are measured in cycle units. The resulting values of the phase shifts, corrected for the presence of recycles, are shown in Fig. 3 as a function of the observation epoch.

The large phase variations, of the order of several cycles in a few hundred days, indicate that input ephemerides of Table 1 are not the best ones and that it is possible to improve them. The corrections, in absence of frequency irregularities, can be obtained by fitting the phase lags by the simple third-degree spin-down model:

$$\Delta\phi(t) = \Delta\nu_o(t-t_0) + \frac{1}{2}\Delta\dot{\nu}_o(t-t_0)^2 + \frac{1}{6}\Delta\ddot{\nu}_o(t-t_0)^3, \quad (2)$$

where $\Delta\phi(t)$ is the measured phase difference at time t , t_0 is the reference epoch and $\Delta\nu_o$, $\Delta\dot{\nu}_o$, $\Delta\ddot{\nu}_o$ are the

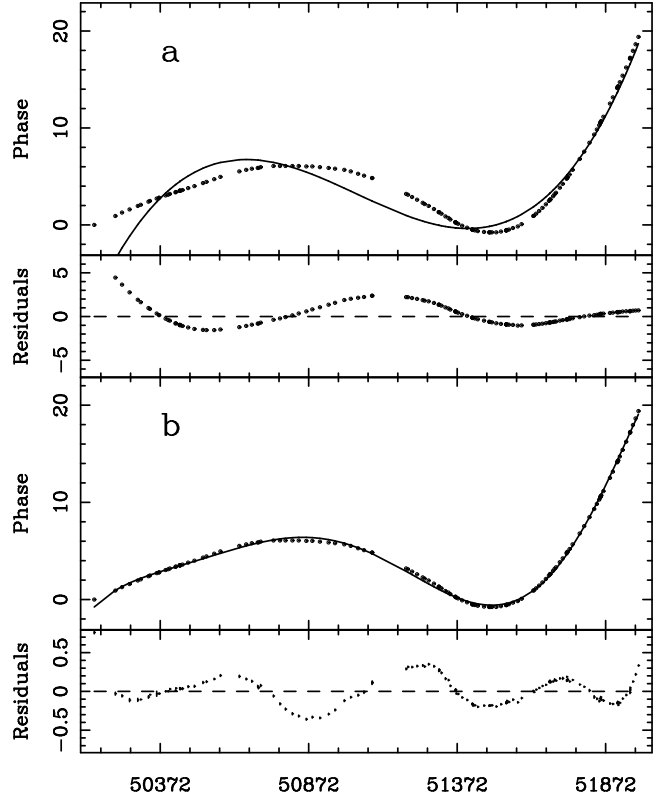


Fig. 3. Phase of the pulsed signal, after a careful reconstruction of the phase recycles for the entire set of the RXTE observations, vs observing time. Phase is in cycle units. Panel *a* shows the fit with a third order polynomial and panel *b* shows the fit with a sixth order polynomial. Data and fitting models are shown in the top, residuals in the bottom.

ephemeris corrections for the frequency, first and second derivatives, respectively. We found that this equation fails to describe the entire set of phase data showing very large systematic deviations (panel *a* of Fig. 3). Such deviations indicate the presence of a timing noise characteristic of several other pulsars (Arzoumanian et al. 1994, Lyne 1999). We tried also to correct the phases by fitting higher order polynomials, up to the sixth degree. The best fit for this model is shown in the panel *b* of Fig. 3: the residuals are of course largely reduced with respect to the other fit and the general behaviour is much better described, but smaller amplitude systematic deviations remain apparent.

To quantify the timing noise we can calculate the Δ_8 parameter defined by Arzoumanian et al. (1994) as:

$$\Delta_8 = \log(10^{24}|\ddot{\nu}|/6\nu). \quad (3)$$

For PSR 0540–69 instead of the measured $\ddot{\nu}$, whose large value is related to the regular spin down rather than the timing noise, we used the correction that takes into account the residuals shown in Fig. 3a. A reliable estimate of this correction is given by the difference between the third degree coefficient of the best fit parameters of the sixth and third degree polynomials. This difference was found equal to $2.27 \times 10^{-22} \text{ Hz s}^{-2}$ and gives $\Delta_8=0.28$,

Table 1. Ephemerides of PSR B0540–69 obtained from a second-degree polynomial fit of the frequency data sets reported in Table A1. 1σ error is given in parentheses for the corresponding last significant digits.

Data Set	t_0 (MJD)	ν (Hz)	$\dot{\nu}$ ($\times 10^{-10}$ Hz s $^{-1}$)	$\ddot{\nu}$ ($\times 10^{-21}$ Hz s $^{-2}$)
ASCA+BeppoSAX	50372.5481748585	19.81583115(7)	-1.880724(7)	3.74(2)
RXTE	50372.5481748585	19.8158314(1)	-1.8808(1)	3.73(20)
ASCA+BeppoSAX+RXTE	50372.5481748585	19.81583119(4)	-1.880727(8)	3.717(7)

higher than all the values of the sample of Arzoumanian et al. (1994). Note that PSR B0540-69 lies well in the upper part of the plot Δ_8 vs \dot{P} given by these authors.

For comparing our results with those of Zhang et al. (2001) we divided our data into two subsets, before and after the time of the glitch, assumed at MJD 51325 – the interval of possible epochs given by Zhang et al. (2001), spans 45 days – and applied a cubic polynomial fit to each subset. We obtained acceptable fits, characterized by nearly zero residuals; resulting best fit values for the two intervals are reported in Table 2, the ephemerides are given in Table 3. Propagating the parameters of Table 3 to the epoch of the glitch we obtained a marginal detection for the frequency change $\Delta\nu/\nu = (1.8 \pm 1.0) \times 10^{-9}$, whereas more significant differences were found for the first and second derivative: $\Delta\dot{\nu}/\dot{\nu} = (1.69 \pm 0.01) \times 10^{-4}$ and $\Delta\ddot{\nu}/\ddot{\nu} = (2.043 \pm 0.001) \times 10^{-3}$. The significance of these parameters’ differences can be largely affected by the timing noise systematics. To verify this hypothesis we performed a similar analysis on other data subsets selected by changing the separation epochs and values of $\Delta\nu/\nu$ of the same order and similar significance were found. This last finding addressed us to interpret the marginal detection of frequency jump at the glitch epoch claimed by Zhang et al. (2001) as a not genuine result but due to the pulse phase analysis in presence of strong timing noise.

3.3. The braking index

As discussed in the Introduction, a relevant difference between our previous results (Mineo et al. 1999) and those of Zhang et al. (2001) is in the value of the braking index: we essentially confirmed the estimates of Deeter et al. (1998), Hirayama et al. (2002), while Zhang et al. (2001) gave the value of 1.81, about 14% smaller, but significantly different when considering the associated uncertainties. Using the new ephemerides given in Table 3, we computed for the two intervals the values of n and obtained 2.1272 ± 0.0003 and 2.122 ± 0.001 for the first and second interval, respectively.

A change in the timing parameters implies a variation of the braking index:

$$\frac{\Delta n}{n} = \frac{\Delta\nu}{\nu} - 2\frac{\Delta\dot{\nu}}{\dot{\nu}} + \frac{\Delta\ddot{\nu}}{\ddot{\nu}}. \quad (4)$$

From the above results it is clear that the parameter responsible for the much lower value of n measured by Zhang et al. (2001) is the second frequency derivative, for which

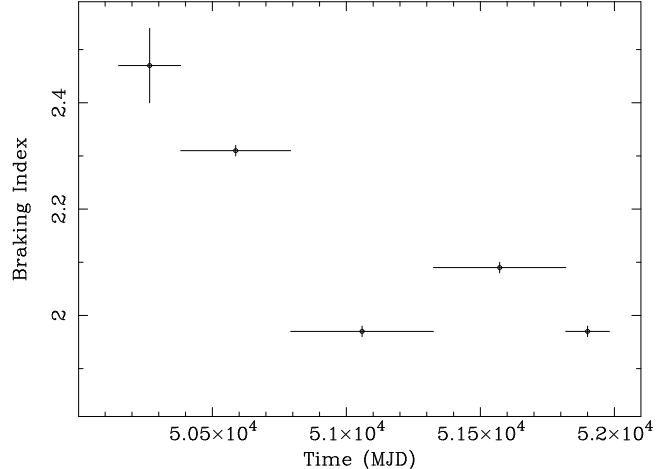


Fig. 4. The values of the braking index computed in several intervals plotted as a function of the central time of the interval. These large changes are a consequence of the timing noise affecting the second derivative of the pulsar frequency.

these authors reported the value of $(3.23 \pm 0.12) \times 10^{-21}$ s $^{-2}$, just 15% smaller than our result.

This discrepancy is likely due to the presence of such high timing noise, because the data set considered by Zhang et al. (2001) spans a rather narrow time interval with respect to that considered by us. To further investigate this point we computed the braking index in several independent time intervals, evaluating the best corrections to the pulsar ephemerides in each of them. The resulting values are shown in Fig. 4: they range from 1.97 to 2.47. Again the largest variation is due to the estimates of second derivative of the pulsar frequency, which differs of $\sim 20\%$, between the various intervals. We conclude, that reliable estimates of the braking index can be obtained only considering the longest time intervals in which a good fit of phases (or TOA) with Eq.(2) can be obtained, likely spanning several years. The use of shorter intervals can introduce a bias due to the timing noise.

4. Discussion

The only way to study the timing noise of PSR B0540-69 is the use of a dense set of X-ray observations, like that of RXTE, because this young pulsar is in the Large Magellanic Cloud and its flux is too weak to be monitored in the radio band. Our analysis on a large database of X-ray observations of PSR B0540-69, covering more than 5

Table 2. Corrections to the timing parameters of PSR B0540–69.

Time Interval	$\Delta\nu$ (Hz)	$\Delta\dot{\nu}$ (Hz s ⁻¹)	$\Delta\ddot{\nu}$ (Hz s ⁻²)
(1) $t < 51325$ MJD	$-1.359(2) \times 10^{-7}$	$1.68(2) \times 10^{-15}$	$8.00(4) \times 10^{-23}$
(2) $t > 51325$ MJD	$2.487(9) \times 10^{-6}$	$-2.94(2) \times 10^{-14}$	$7.2(2) \times 10^{-23}$

Table 3. Frequency ephemerides obtained from a phase coherent analysis before and after MJD 51325

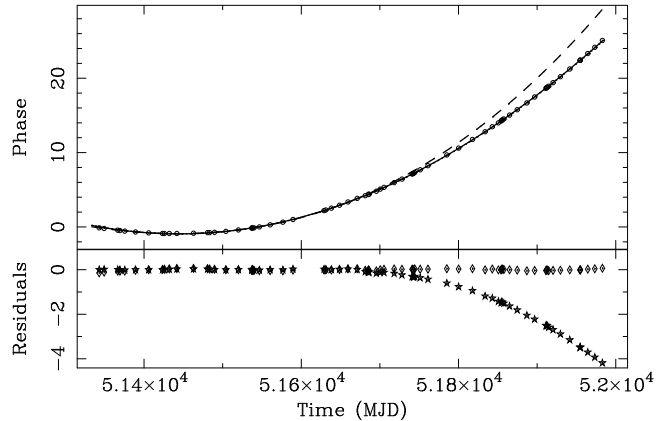
Time Interval	t_0 (MJD)	ν (Hz)	$\dot{\nu}$ ($\times 10^{-10}$ Hz s ⁻¹)	$\ddot{\nu}$ ($\times 10^{-21}$ Hz s ⁻²)	n
(1) $t < 51325$ MJD	50372.5481748585	19.8158310541(2)	-1.8807101(2)	3.7970(4)	2.1272(3)
(2) $t > 51325$ MJD	50372.5481748585	19.815833677(9)	-1.881021(2)	3.789(2)	2.122(1)

years, provided a good evidence for a relevant timing noise affecting the phase of the pulsed signal. In particular, we showed that the best fit of a third degree polynomial, including up to the second frequency derivative, gives phase residuals up to a few cycles and that residuals as large as 0.4 remain even when a sixth degree polynomial is used. Assuming that the difference in the second derivative obtained from these best fits is a measure of its fluctuations, we evaluated the Δ_8 parameter (Arzoumanian et al.1994) which was found equal to 0.28, confirming the high level of timing noise. Taking into account that even larger variations of this derivative are also found when polynomial best fits are performed over shorter time intervals, this result could be considered a lower limit. Furthermore, it supports the finding that timing noise is stronger in young pulsars with a high \dot{P} .

A consequence of this high timing noise is that the glitch claimed by Zhang et al. (2001) cannot be confirmed. The frequency difference of this event given by these authors is very small, about $0.04 \mu\text{Hz}$. The glitch cannot be detected directly as a sudden frequency jump because it is quite less than the uncertainties in the frequency measurements which are typically of the order of a few μHz , and in the best conditions of a few tenth of μHz . Zhang et al. (2001) also excluded that this effect can be due to timing noise, but their conclusion is affected by the use of a shorter time interval that does not allows an accurate analysis of the timing noise.

At variance, our results show that frequency differences of the same order of that given by Zhang et al. (2001) are usually found when different selections of time intervals are considered and they do not depend upon a well defined episode.

From the timing noise analysis we were also able to show how much the first and second derivative of the pulsar frequency are stable in time. We found that the former can have fluctuations of amplitude of about 10^{-4} , while for the latter fluctuations can be much higher, and in some cases the estimates can differ of ~ 10 – 20% , depending upon the length of the time interval taken into account. Such large variations affect the evaluation of the braking index, particularly when it is found by the fitting of Eq.(2) to the pulse phases. We showed that when

**Fig. 5.** Phase residuals obtained extrapolating the ephemerides solution of Zhang et al. (2001) to the entire subset of data after the epoch MJD 51325.

the longest possible intervals are considered, n turns out to be very close to 2.12, in agreement with several other previous estimates, while values as that given by Zhang et al. (2001) are obtained in shorter intervals. We verified this interpretation by fitting Eq.(2) to the same subset of RXTE observations used by these authors (more specifically, the fit was performed on RXTE observations from row 82 to row 114 of Table A1) and derived from the best fit ephemeris $n = 1.854 \pm 0.003$. However, when these parameters are used to extrapolate the phase shift to the entire subset data after the epoch of the glitch claimed by Zhang et al. (2001) they produce a systematic deviation of the residuals which increases with the elapsed time, as shown in plot of Fig. 5.

Finally, we note that the agreement of our estimate of braking index with those derived from ASCA (Hirayama et al. 2002) and BeppoSAX (Mineo et al. 1999) data can be easily understood on the basis of the rather long time intervals covered by the observations. They are too sparse to provide a good information on the timing noise but can give a right evaluation of the mean second derivative.

Acknowledgements. The authors are very grateful to the referee, R.N.Manchester, for the relevant comments and suggestions that greatly improved the scientific content of the paper.

This work has been partially supported by the Italian Space Agency (ASI).

References

- Arzoumanian Z., Nice D. J., Taylor J. H., Thorsett S. E., 1994, *ApJ* 422, 671
- Boella G., Butler R.C., Perola G.C., et al., 1997a, *A&AS* 122, 299
- Boella G., Chiappetti L., Conti G., et al., 1997b, *A&AS* 122, 327
- Boyd P.T., van Citters G.W., Dolan J.F., et al., 1995, *ApJ* 448, 365
- Caraveo P.A., Bignami, G.F., Mereghetti, S., Mombelli, M., 1992, *ApJ* 395, L103
- Deeter J.E., Nagase F., Boyton P.E., 1999, *ApJ* 512, 300
- Hirayama M., Nagase F., Gunji S., Sekimoto Y., Saito Y., 1996, *ASCANews*, Issue 4, 18
- Hirayama M., Nagase F., Endo T., Kawai N., Itoh M., 2002, *MNRAS* 333, 603
- Lyne A., 1999, on proceedings of the colloquium, Amsterdam "Pulsar Timing, General Relativity and the Internal Structure of Neutron Stars", 24-27 September 1996
- Makishima, K., Tashiro, M., Ebisawa, K., et al., 1996, *PASJ* 48, 171
- Manchester R.N., Peterson B.A., 1989, *ApJ* 342, L23
- Manchester R.N., Mar D.P., Lyne A.G., Kaspi V.M., Johnston S., 1993, *ApJ* 403, L29
- Middleditch J., Pennypacker C.R., 1985, *Nat* 313, 659
- Mineo, T., Cusumano, G., Massaro, E. et al., 1999, *A&A* 348, 519
- Nagase F., Deeter J., Lewis W., Donati T., Makino K., Mitsuda K., 1990, *ApJ* 351, L13
- Ögelman H., Hasinger G., 1990, *ApJ* 353, L21
- Ohashi, T., Ebisawa, K., Fukazawa, Y., et al., 1996, *PASJ* 48, 157O
- Seward F.D., Harnden F.R., Helfand D.J., 1984, *ApJ* 287, L19
- Standish E. M., 1982, *A&A*, 114, 297
- Tanaka, Y., Inoue, H., Holt, S.S., 1994, *PASJ* 46, L37
- Wong T., Backer D.C., Lyne A.G. 2001, *ApJ* 548, 447
- Zhang, W.; Marshall, F. E.; Gotthelf, E. V., et al., 2001, *ApJ* 554, 177

Appendix

In this appendix we report a table containing the central epoch of the observation (column 2), the total duration (column 3), exposure time (column 4), TOA and error (column 5 and 6; only for RXTE observations) and the frequency with the relative error (column 6,7) for each observation analyzed.

Table A1. Observation log and frequency measurements

	Tc (MJD)	Tobservation (s)	Texposure (s)	TOA (MJD)	Err (μ s)	Frequency (Hz)	Err (Hz)
ASCA							
1	49151.8084349484	89463	30852			19.83568828	2.4×10^{-7}
2	49220.5355756515	94816	32141			19.83456882	5.0×10^{-7}
3	49252.0870520244	64656	23294			19.83405527	5.5×10^{-7}
4	49254.4624576429	82879	35572			19.83401684	1.4×10^{-7}
5	49626.1810950798	32480	11504			19.82796873	7.0×10^{-7}
6	49628.1308000431	24529	91460			19.82793815	9.5×10^{-7}
7	49636.3810082158	14688	10550			19.8278009	1.9×10^{-6}
8	49637.7172262562	14996	93339			19.8277789	1.6×10^{-6}
9	49663.2073326372	14606	38299			19.8273641	3.1×10^{-6}
10	50028.4455501792	1866565	72232			19.82142441	2.0×10^{-7}
11	50395.3696804385	2422872	90891			19.815460211	9.2×10^{-8}
12	50759.8892585014	1638235	71682			19.80953905	1.2×10^{-7}
13	51121.2406563684	2135813	85952			19.80367343	1.5×10^{-7}
14	51485.0385356526	2183033	89302			19.797770995	8.4×10^{-8}
SAX							
15	50382.3304918242	71318	38347			19.81567247	2.6×10^{-7}
16	50727.1972055422	55830	36233			19.81007055	8.5×10^{-7}
17	51463.4493485718	52119	23390			19.79812490	9.6×10^{-7}
18	51465.3785121305	39908	15803			19.79808990	3.0×10^{-7}
19	51593.2879147687	50285	28160			19.79601371	9.2×10^{-7}
RXTE							
20	50150.2775566760	7321	4953	50150.2775569566	915	19.8194548	7.0×10^{-6}
21	50221.3528223318	6622	4921	50221.3528227907	937	19.8182871	7.2×10^{-6}
22	50243.8885962850	6698	4991	50243.8885964943	705	19.8179247	6.1×10^{-6}
23	50269.1237492340	6992	4623	50269.1237493630	1019	19.817515	1.1×10^{-5}
24	50296.9179287483	7043	4991	50296.9179291788	999	19.8170510	8.7×10^{-6}
25	50306.7631433992	13935	11614	50306.7631436463	233	19.8169009	1.1×10^{-6}
26	50332.9466234517	6869	4926	50332.9466237179	752	19.8164739	6.5×10^{-6}
27	50337.8103624822	19359	11791	50337.8103627079	231	19.81639654	7.6×10^{-7}
28	50360.5331308203	1517	1517	50360.5331308787	1634	19.8160378	1.6×10^{-6}
29	50368.4418745432	50495	31966	50368.4418750643	193	19.81589787	2.2×10^{-7}
30	50390.7548928533	12799	8719	50390.7548930179	300	19.8155341	1.6×10^{-6}
31	50399.2989191193	19839	9422	50399.2989195186	295	19.81539563	9.3×10^{-7}
32	50404.8100013632	13247	5870	50404.8100015330	420	19.8153074	2.07×10^{-6}
33	50423.9342602285	110991	82523	50423.9342607360	206	19.81499676	3.7×10^{-7}
34	50425.2694394845	115631	90731	50425.2694396661	278	19.81497489	4.2×10^{-7}
35	50437.9618005898	71055	32169	50437.9618006700	249	19.81476840	2.4×10^{-7}
36	50438.7223552708	39727	23565	50438.7223552489	253	19.81475603	4.5×10^{-7}
37	50439.2099444506	28303	10061	50439.2099444447	407	19.81474798	8.9×10^{-7}
38	50439.5834629385	17679	10703	50439.5834632837	390	19.8147411	1.4×10^{-6}
39	50447.5335356081	15871	9774	50447.5335359889	602	19.8146102	2.6×10^{-6}
40	50466.4364738898	14495	9823	50466.4364740499	567	19.8143005	2.4×10^{-6}
41	50487.4681557080	14911	9695	50487.4681561890	620	19.8139646	3.2×10^{-6}
42	50516.4543557125	16959	10031	50516.4543557915	662	19.8134923	2.7×10^{-6}
43	50528.1082981453	17119	10511	50528.1082981650	518	19.8133003	2.2×10^{-6}
44	50554.2917732432	17119	10511	50554.2917735571	457	19.8128801	1.9×10^{-6}
45	50575.1344847706	9855	7391	50575.1344850982	576	19.8125484	3.7×10^{-6}
46	50617.1578258350	8511	5135	50617.1578260369	703	19.8118621	4.3×10^{-6}
47	50638.6538020237	9215	4302	50638.6538022807	716	19.8115068	5.2×10^{-6}
48	50661.8875122125	9215	4302	50661.8875124521	563	19.8111311	2.9×10^{-6}
49	50680.8301644068	13743	9087	50680.8301645705	623	19.8108234	2.9×10^{-6}
50	50700.8130593871	18991	9998	50700.8130594987	655	19.8104987	2.2×10^{-6}
51	50703.1069385382	14671	9487	50703.1069386272	670	19.8104571	2.4×10^{-6}
52	50710.7365335916	17359	9710	50710.7365336879	668	19.8103351	3.0×10^{-6}
53	50731.7088303996	15983	11311	50731.7088308387	597	19.8099983	2.5×10^{-6}
54	50753.7282404459	14175	9023	50753.7282405495	628	19.8096421	2.8×10^{-6}
55	50775.6616390784	14367	8335	50775.6616392198	663	19.8092816	2.7×10^{-6}
56	50794.3808143453	14303	9631	50794.3808147188	610	19.8089757	2.7×10^{-6}
57	50817.4650993146	13295	9359	50817.4651097875	679	19.8086047	3.0×10^{-6}
58	50838.7500841077	13103	9871	50838.7500840900	599	19.8082568	3.3×10^{-6}
59	50864.4661456054	13103	9871	50864.4661458375	606	19.8078396	2.5×10^{-6}

Table A1 (continued).

	Tc (MJD)	Tobservation (s)	Texposure (s)	TOA (MJD)	Err (μ s)	Frequency (Hz)	Err (Hz)
60	50884.6064968517	18991	9758	50884.6064972624	570	19.8075165	2.0×10^{-6}
61	50910.3122764558	14784	9583	50910.3122764554	516	19.8070939	2.4×10^{-6}
62	50939.2524410826	15999	11263	50939.2524415522	504	19.8066292	2.0×10^{-6}
63	50961.2281108092	21087	9903	50961.2281108402	612	19.8062677	1.6×10^{-6}
64	50992.1907233621	14255	9807	50992.1907237746	540	19.8057660	2.4×10^{-6}
65	51014.0147368956	17791	9967	51014.0147372862	510	19.8054145	1.7×10^{-6}
66	51038.8493459019	13343	9215	51038.8493458773	599	19.8050143	3.0×10^{-6}
67	51058.7992902631	13471	9263	51058.7992908122	768	19.8046821	3.3×10^{-6}
68	51085.8265752465	9567	7167	51085.8265753553	901	19.8042484	4.8×10^{-6}
69	51086.5263870566	3839	3023	51086.5263874268	931	19.8042625	1.8×10^{-5}
70	51200.6063583254	8331	5013	51200.6063586919	569	19.8023902	3.7×10^{-6}
71	51206.7338605356	6939	5235	51206.7338608225	455	19.8022809	4.0×10^{-6}
72	51220.4579412823	7461	4927	51220.4579415977	472	19.8020643	3.5×10^{-6}
73	51237.3581160727	12119	5575	51237.3581160859	523	19.8017889	2.9×10^{-6}
74	51256.4577562548	7275	5101	51256.4577562472	485	19.8014780	3.9×10^{-6}
75	51262.6929378694	4917	4917	51262.6929381281	417	19.8013909	6.1×10^{-6}
76	51276.3248166093	12745	4772	51276.3248166847	500	19.8011557	2.3×10^{-6}
77	51294.1430088117	8059	4919	51294.1430087889	548	19.8008694	3.9×10^{-6}
78	51310.5136331496	7286	4963	51310.5136331665	404	19.8006079	4.1×10^{-6}
79	51310.8142483174	7286	4963	51310.8142483560	491	19.8005952	3.9×10^{-6}
80	51311.5969028145	4760	4760	51311.5969030305	523	19.8005936	6.7×10^{-6}
81	51319.3224291899	6599	4893	51319.3224294960	555	19.8004542	6.4×10^{-6}
82	51333.0588017849	8845	5461	51333.0588019978	594	19.8002358	3.4×10^{-6}
83	51342.9771166913	8328	4895	51342.9771167629	417	19.8000736	2.5×10^{-6}
84	51349.2476702360	8259	4585	51349.2476704655	453	19.7999788	3.0×10^{-6}
85	51366.0873172747	8136	5949	51366.0873174558	443	19.7996991	3.2×10^{-6}
86	51366.2957090773	7646	5943	51366.2957094965	450	19.7996941	3.6×10^{-6}
87	51367.0866244652	8135	5955	51367.0866245036	455	19.7996833	3.7×10^{-6}
88	51369.3537227011	6981	6003	51369.3537228107	427	19.7996450	3.7×10^{-6}
89	51375.5511251919	6707	6707	51375.5511254046	404	19.7995450	3.8×10^{-6}
90	51389.1947032382	6861	4965	51389.1947032309	436	19.7993291	4.0×10^{-6}
91	51405.9278060073	7493	4899	51405.9278063126	443	19.7990606	3.4×10^{-6}
92	51422.9600145157	7493	4899	51422.9600149667	421	19.7987815	4.0×10^{-6}
93	51423.2303145269	7175	5055	51423.2303149586	426	19.7987702	3.6×10^{-6}
94	51423.8219443136	8381	6201	51423.8219447693	384	19.7987638	2.7×10^{-6}
95	51425.8291939941	10127	8005	51425.8291944455	334	19.7987333	1.9×10^{-6}
96	51432.0903727191	6151	4875	51432.0903732235	380	19.7986228	3.7×10^{-6}
97	51441.7468451228	8865	5683	51441.7468456561	380	19.7984691	2.4×10^{-6}
98	51462.9139902142	18963	5107	51462.9139906137	438	19.7981279	1.4×10^{-6}
99	51480.3046770383	5075	5076	51480.3046775678	434	19.7978457	6.4×10^{-6}
100	51481.2968009249	5951	5027	51481.2968014625	428	19.7978231	6.1×10^{-6}
101	51483.3334558311	10179	6398	51483.3334558612	357	19.7977987	2.2×10^{-6}
102	51489.6844611122	8919	6137	51489.6844614279	423	19.7976958	2.6×10^{-6}
103	51504.0707028282	18843	4896	51504.0707030781	418	19.7974617	1.3×10^{-6}
104	51519.9853613432	6697	5055	51519.9853617755	413	19.7971995	3.6×10^{-6}
105	51537.0292132529	7509	5801	51537.0292133426	391	19.7969327	3.3×10^{-6}
106	51537.4694203451	8597	5263	51537.4694203866	479	19.7969234	3.2×10^{-6}
107	51537.9957500760	6211	4811	51537.9957503765	449	19.7969143	4.9×10^{-6}
108	51539.7908841811	7291	4971	51539.7908846815	395	19.7968813	3.5×10^{-6}
109	51546.7092482877	10125	5153	51546.7092487340	438	19.7967703	3.1×10^{-6}
110	51560.3473796373	8443	5003	51560.3473898280	463	19.7965521	3.3×10^{-6}
111	51576.6172108713	7293	5349	51576.6172111729	451	19.7962743	4.5×10^{-6}
112	51589.4437727056	8107	5453	51589.4437728199	463	19.7960736	3.2×10^{-6}
113	51628.7753839364	12515	7247	51628.7753839364	396	19.7954385	1.8×10^{-6}
114	51631.2044355514	28857	8645	51631.2044357594	329	19.79540002	6.9×10^{-7}
115	51638.3028766256	19173	7803	51638.3028766256	345	19.7952859	1.1×10^{-6}
116	51648.5466267813	17863	7297	51648.5466272009	370	19.7951216	1.4×10^{-6}
117	51659.3677297694	14227	7883	51659.3677301986	349	19.7949445	1.7×10^{-6}
118	51671.1320448646	12725	8077	51671.1320448645	344	19.7947566	1.7×10^{-6}

Table A1 (continued).

	Tc (MJD)	Tobservation (s)	Texposure (s)	TOA (MJD)	Err (μ s)	Frequency (Hz)	Err (Hz)
119	51681.3454690879	18336	8181	51681.3454692289	420	19.7945862	1.3×10^{-6}
120	51684.7731936208	4788	2699	51684.7731939477	686	19.7945483	9.2×10^{-6}
121	51685.3175718948	20279	8857	51685.3175720315	324	19.79452255	9.6×10^{-7}
122	51686.2075746935	14087	7361	51686.2075748901	364	19.7945075	1.4×10^{-6}
123	51695.4979676551	8675	6585	51695.4979680772	424	19.7943538	3.0×10^{-6}
124	51705.1979969286	9037	7093	51705.1979970477	349	19.7942000	2.4×10^{-6}
125	51728.0434880623	8267	5424	51728.0434883792	659	19.7938357	4.9×10^{-6}
126	51740.9588341276	14019	8041	51740.9588343721	586	19.7936227	2.5×10^{-6}
127	51741.7215067928	9785	7727	51741.7215072644	355	19.7936115	2.1×10^{-6}
128	51742.8596909607	9907	7733	51742.8596914658	333	19.7935918	2.0×10^{-6}
129	51744.2896447745	13735	7827	51744.2896451619	333	19.7935685	1.6×10^{-6}
130	51751.1810596555	9819	8123	51751.1810597295	331	19.7934563	2.1×10^{-6}
131	51761.1185637994	13057	7771	51761.1185642818	322	19.7932910	1.5×10^{-6}
132	51785.0980336962	24995	9013	51785.0980341569	307	19.79290630	7.2×10^{-7}
133	51800.1416986946	8874	7731	51800.1416989359	341	19.7926609	2.3×10^{-6}
134	51817.7362062067	7231	5409	51817.7362064879	683	19.7923712	7.2×10^{-6}
135	51833.7908365378	8432	5217	51833.7908366692	822	19.7921206	5.0×10^{-6}
136	51842.9466249313	18462	8713	51842.9466252357	509	19.7919684	1.9×10^{-6}
137	51850.7533332734	12975	8503	51850.7533333821	520	19.7918429	2.3×10^{-6}
138	51854.1343244782	12300	8261	51854.1343246987	337	19.7917833	1.8×10^{-6}
139	51854.7806751278	9334	7205	51854.7806753799	389	19.7917757	2.1×10^{-6}
140	51855.7761402855	9391	7379	51855.7761404915	359	19.7917586	2.2×10^{-6}
141	51857.6643855983	14666	7715	51857.6643857372	372	19.7917283	1.7×10^{-6}
142	51864.8967614676	3471	7215	51864.8967616390	467	19.791594	1.0×10^{-5}
143	51886.9135988688	10217	8413	51886.9135993413	460	19.7912528	2.5×10^{-6}
144	51896.8522715505	8927	5353	51896.8522718532	382	19.7910941	2.4×10^{-6}
145	51911.2433041537	19227	6145	51911.2433043693	415	19.7908604	1.2×10^{-6}
146	51911.8487562932	9263	7181	51911.8487567141	397	19.7908517	2.5×10^{-6}
147	51912.8241077159	12570	7301	51912.8241078523	388	19.7908334	2.0×10^{-6}
148	51914.6370942449	8584	6203	51914.6370947508	355	19.7908040	2.3×10^{-6}
149	51920.2291815557	13749	5932	51920.2291819350	444	19.7907147	1.9×10^{-6}
150	51929.5870831782	14465	7573	51929.5870831607	378	19.7905631	1.6×10^{-6}
151	51941.4093028956	13340	6081	51941.4093032091	464	19.7903715	2.1×10^{-6}
152	51954.5931647284	12499	7201	51954.5931647444	810	19.790178	4.3×10^{-5}
153	51954.7239382431	12499	7201	51954.7239384635	538	19.7901562	2.0×10^{-6}
154	51954.9246680830	12373	7391	51954.9246684580	596	19.7901536	2.6×10^{-6}
155	51964.4474052025	8564	8118	51964.4474055636	387	19.7900000	2.5×10^{-6}
156	51973.2333393971	24758	9000	51973.2333393914	501	19.789861	1.0×10^{-5}
157	51982.9725223272	25961	7904	51982.9725226691	371	19.78969766	7.8×10^{-7}